



**HAL**  
open science

## Different Pigmentation Risk Loci for High-Risk Monosomy 3 and Low-Risk Disomy 3 Uveal Melanomas

Lenha Mobuchon, Anne-Céline Derrien, Alexandre Houy, Thibault Verrier, Gaëlle Pierron, Nathalie Cassoux, Maud Milder, Jean-François Deleuze, Anne Boland, Josselin Noirel, et al.

► **To cite this version:**

Lenha Mobuchon, Anne-Céline Derrien, Alexandre Houy, Thibault Verrier, Gaëlle Pierron, et al.. Different Pigmentation Risk Loci for High-Risk Monosomy 3 and Low-Risk Disomy 3 Uveal Melanomas. JNCI: Journal of the National Cancer Institute, 2021, 10.1093/jnci/djab167 . hal-03326678

**HAL Id: hal-03326678**

**<https://cnam.hal.science/hal-03326678>**

Submitted on 22 Sep 2021

**HAL** is a multi-disciplinary open access archive for the deposit and dissemination of scientific research documents, whether they are published or not. The documents may come from teaching and research institutions in France or abroad, or from public or private research centers.

L'archive ouverte pluridisciplinaire **HAL**, est destinée au dépôt et à la diffusion de documents scientifiques de niveau recherche, publiés ou non, émanant des établissements d'enseignement et de recherche français ou étrangers, des laboratoires publics ou privés.



Distributed under a Creative Commons Attribution - NonCommercial 4.0 International License

# Different Pigmentation Risk Loci for High-Risk Monosomy 3 and Low-Risk Disomy 3 Uveal Melanomas

Lenha Mobuchon, PhD,<sup>1,†</sup> Anne-Céline Derrien, MSc,<sup>1,†</sup> Alexandre Houy, MSc,<sup>1,†</sup> Thibault Verrier, BSc,<sup>1</sup> Gaëlle Pierron, PhD,<sup>2</sup> Nathalie Cassoux, MD, PhD,<sup>3,4</sup> Maud Milder, MSc,<sup>5</sup> Jean-François Deleuze, PhD,<sup>6</sup> Anne Boland, PhD,<sup>6</sup> Ghislaine Scelo, PhD,<sup>7,8</sup> Géraldine Cancel-Tassin, PhD,<sup>9,10</sup> Olivier Cussenot, MD, PhD,<sup>9,10</sup> Manuel Rodrigues, MD, PhD,<sup>1,11</sup> Josselin Noirel, PhD,<sup>12</sup> Mitchell J. Machiela, PhD,<sup>13</sup> Marc-Henri Stern, MD, PhD,<sup>1,\*</sup>

<sup>1</sup>Inserm U830, DNA Repair and Uveal Melanoma (D.R.U.M.), Equipe labellisée par la Ligue Nationale Contre le Cancer, Institut Curie, PSL Research University, Paris, 75005, France

<sup>2</sup>Somatic Genetic Unit, Department of Genetics, Institut Curie, PSL Research University, Paris, 75005, France

<sup>3</sup>Department of Ocular Oncology, Institut Curie, Paris, 75005, France

<sup>4</sup>Faculty of Medicine, University of Paris Descartes, Paris, 75005, France

<sup>5</sup>Inserm CIC BT 1418, Institut Curie, PSL Research University, Paris, 75005, France

<sup>6</sup>Université Paris-Saclay, CEA, Centre National de Recherche en Génomique Humaine, 91057, Evry, France

<sup>7</sup>International Agency for Research on Cancer (IARC), Lyon, 69372, France

<sup>8</sup>Cancer Epidemiology Unit, Department of Medical Sciences, University of Turin, Turin, Italy

<sup>9</sup>CeRePP, Tenon Hospital, Paris, 75020, France

<sup>10</sup>Sorbonne University, GRC n°5 Predictive Onco-Urology, AP-HP, Tenon Hospital, Paris, 75020, France

<sup>11</sup>Institut Curie, PSL Research University, Department of Medical Oncology, Paris, 75005, France

<sup>12</sup>Laboratoire GBCM (EA7528), CNAM, HESAM Université, Paris, 75003, France

© The Author(s) 2021. Published by Oxford University Press.

This is an Open Access article distributed under the terms of the Creative Commons Attribution Non-Commercial License (<http://creativecommons.org/licenses/by-nc/4.0/>), which permits non-commercial re-use, distribution, and reproduction in any medium, provided the original work is properly cited. For commercial re-use, please contact [journals.permissions@oup.com](mailto:journals.permissions@oup.com)

<sup>13</sup>Division of Cancer Epidemiology and Genetics, National Cancer Institute, Bethesda, MD,  
20892, USA

†These authors contributed equally to this work.

\*Corresponding author:

Marc-Henri Stern, MD, PhD

Institut Curie, Inserm U830

26 rue d'Ulm, 75248 Paris cedex 05, France

Email: [marc-henri.stern@curie.fr](mailto:marc-henri.stern@curie.fr);

Telephone: +33 1 56 24 66 46

## Abstract

**Background.** Uveal melanoma (UM), a rare malignant tumor of the eye, is predominantly observed in populations of European ancestry. UMs carrying a monosomy 3 (M3) frequently relapse mainly in the liver, whereas UMs with disomy 3 (D3) are associated with more favorable outcome. Here, we explored the UM genetic predisposition factors in a large genome-wide association study (GWAS) of 1,142 European UM patients and 882 healthy controls.

**Methods.** We combined two independent datasets (GSA array) with the dataset described in a previously published GWAS in UM (Omni5 array), which were imputed separately and subsequently merged. Patients were stratified according to their chromosome 3 status and identified UM risk loci were tested for differential association with M3 or D3 subgroups. All statistical tests were two-sided.

**Results.** We recapitulated the previously identified risk locus on chromosome 5 on *CLPTM1L* (rs421284: odds ratio [OR] = 1.58, 95% confidence interval [CI] = 1.35-1.86;  $P=1.98\times 10^{-8}$ ) and identified two additional risk loci involved in eye pigmentation: *IRF4* locus on chromosome 6 (rs12203592: OR = 1.76, 95% CI = 1.44-2.16;  $P=3.55\times 10^{-8}$ ) and *HERC* locus on chromosome 15 (rs12913832: OR= 0.57, 95% CI = 0.48-0.67;  $P=1.88\times 10^{-11}$ ). The *IRF4* rs12203592 SNP was found to be exclusively associated with risk for the D3 UM subtype ( $OR_{D3} = 2.73$ , 95% CI = 1.87-3.97;  $P=1.78\times 10^{-7}$ ), and the *HERC2* rs12913832 SNP was exclusively associated with risk for the M3 UM subtype ( $OR_{M3} = 2.43$ , 95% CI = 1.79-3.29;  $P=1.13\times 10^{-8}$ ). However, the *CLPTM1L* risk locus was equally statistically significant in both subgroups.

**Conclusion.** This work identified two additional UM risk loci known for their role in pigmentation. Importantly, we demonstrate that UM tumor biology and metastatic potential are influenced by patients' genetic backgrounds.

**Keywords:** uveal melanoma, GWAS, pigmentation

Uveal melanoma (UM) arises from melanocytes in the uveal tract of the eye, including the choroid and, more rarely, ciliary body and iris. Prognosis is dismal when the disease spreads, frequently metastasizing to the liver (1). Loss of chromosome 3 and gain of chromosome 8 are associated with a higher risk of metastatic relapse (2,3). Monosomy 3 (M3) UMs are associated with *BAP1* (3p21) mutations and a high risk of metastases (4). Conversely, disomy 3 (D3) tumors carry *SF3B1* or *EIF1AX* mutations (5-7), and are associated with late metastases and a better prognosis. These M3 and D3 subtypes are not only different in terms of mutational statuses, but also at the cytogenetic, miRNome, methylome and proteome levels, suggesting that they derive from two different tumorigenic processes (8).

UM mainly affects populations of European ancestry, with a 10-fold lower incidence in individuals of African-American or Asian/Pacific Islander ancestry (9,10). Fair skin and blue/gray eyes are also risk factors for UM (11). With the hypothesis that higher frequency of risk alleles exists in populations of European ancestry to explain UM epidemiology, we performed the first genome-wide association study (GWAS) in UM and identified rs421284 as the leading SNP on the *CLPTM1L/TERT* risk locus on chromosome 5p15.33. Moreover, a trend for association between variants in *OCA2* and UM was also observed (12). Recently, another UM GWAS identified 11 loci with a p-value of association less than  $10^{-5}$ , but none reached statistical significance (13).

The *CLPTM1L* risk allele identified by our first UM GWAS had a higher frequency in individuals of African-American ancestry compared to Europeans, and thus could not explain the peculiar prevalence of UM in individuals of European ancestry (12). To identify additional UM risk loci in the European population, we increased the power of our GWAS by performing genome-wide genetic imputation and by accruing a total of 1,142 UM cases and 882 controls, a 3-fold increase of our first study, allowing subgroup analysis depending on chromosome 3 status.

## Methods

### Study populations

This study was approved by the Ethical Committee and Internal Review Board at the Institut Curie. Blood samples were obtained from 946 UM patients who consented to participate to the study and from 496 control individuals of French origin from the KIDRISK consortium (US NCI U01CA155309; G. Scelo). Genotypes obtained on the Infinium Global Screening Array 24 v1.0 were called using default parameters in GenomeStudio (Illumina).

### Genotyping, imputation and merge

Genotypes from the previously published GWAS (dataset1) (12), and for the two new sets (dataset2 and dataset3) were filtered (**Supplementary Methods**), and independently imputed on the Michigan Imputation Server using Eagle for the phasing and Haplotype Reference Consortium r1.1 as the reference dataset. Imputed datasets were merged together, and another quality control was performed (**Supplementary Table 1**). Manual genotyping was also performed on selected SNPs and individuals (**Supplementary Methods**). Cases and controls of European ancestry were stringently selected for further analyses (**Supplementary Methods, Supplementary Figures 1 and 2**).

### Statistical analysis

For GWAS, Firth logistic regression was performed using plink2 with covariates described in the **Supplementary Methods**. Exact number of cases and controls used are indicated in the respective figures and tables for each analysis. Association of SNPs with UM risk was determined by odds ratios (ORs) with 95% confidence intervals (CIs), and SNPs with a  $P$  value  $<5.00 \times 10^{-8}$  were considered to be statistically significant while those with  $P$  value  $<1.00 \times 10^{-5}$  only reached the tendency line. Eye color was predicted using IrisPlex tools

(<https://hirisplex.erasmusmc.nl/>). Association of eye color with UM risk was calculated using a two-sided Fisher test p-value and OR. Comparison of Variant Allele Frequency (VAF) of SNPs in different populations were tested for statistical significance using a two-sided Fisher test p-value. Expression Quantitative Trait Loci (eQTL) were performed using linear regression. A *P* value of <0.05 was considered statistically significant for all tests other than GWAS Firth logistic regression.

## Results

### Genome-wide association study in UM

We combined two independent datasets (dataset2: 369 UM and 496 controls; dataset3: 577 UM, GSA array) with that of our previous UM GWAS (dataset1 of 271 UM and 429 controls; Omni5 array) (12). The data were quality filtered (**Figure 1** and **Supplementary Table 1**). The three datasets were imputed separately using the Haplotype Reference Consortium on the Michigan server and subsequently merged. Quality of the genotyping and imputation was further assessed by TaqMan genotyping on rs421284, rs12203592 and rs12913832 SNPs on 972 selected samples, with 95.2%, 99.1% and 99.6% of good match, respectively (**Supplementary Table 2**). Data from individuals of European ancestry were stringently selected from Principal Component Analyses (PCA) using plink2, in which the first two principal components were used. Outliers were then excluded from those selected samples using SmartPCA with 10 iterative PCAs (**Supplementary Figures 1-3**). The final dataset for the UM GWAS analysis consisted of 7,488,175 SNPs in 1,142 cases and 882 controls (**Figure 1**).

The GWAS Manhattan plot showed three distinct loci reaching genome-wide significance (Firth logistic regression  $P < 5.00 \times 10^{-8}$ ) (chr5, *CLPTM1L/TERT* locus; chr6, *IRF4* locus; and chr15, *HERC2/OCA2* locus) (**Figure 2, Supplementary Table 3**). Within the *HERC2/OCA2* locus, 8 SNPs in high linkage disequilibrium (LD) reached statistical

significance. The most statistically significant SNPs at this locus were rs1129038 and rs12913832 (OR = 0.56, 95% CI = 0.48-0.66,  $P=5.97\times 10^{-12}$ ; and OR=0.57, 95% CI = 0.48-0.67,  $P=1.88\times 10^{-11}$ ; respectively), located in *HERC2*. A single SNP located in *IRF4* was found to be well above the genome-wide significance: rs12203592 (OR=1.76, 95% CI= 1.44-2.16,  $P=3.55\times 10^{-8}$ ). Finally, the association study recapitulated the previously identified 5p15.33 risk locus (*TERT/CLPTM1L*) (12), with several SNPs in high LD ( $r^2>0.9$ ) reaching statistical significance (**Supplementary Table 3**). The most statistically significant SNP was rs370348 (OR=1.59, 95% CI = 1.35-1.86,  $P=1.48\times 10^{-8}$ ). rs421284, the leading risk SNP in our first GWAS (12), also showed high statistical significance (OR=1.58, 95% CI = 1.35-1.86,  $P=1.98\times 10^{-8}$ ) and was further analyzed in this study. A few other loci showed suggestive evidence for an association with UM but did not reach genome-wide significance ( $P<5\times 10^{-8}$ ) (**Supplementary Table 3 and Figure 2**).

Conditional analyses enable the detection of secondary independent association signals within a genomic locus by conditioning on the primary associated SNP at the locus. At the *CLPTM1L*, *IRF4* and *HERC2* loci, no other statistically significant SNP was found to be independently associated with UM when conditioning on rs421284, rs12203592, or rs12913832, respectively. Moreover, these three conditional analyses did not reveal any statistically significant regions other than *CLPTM1L*, *IRF4*, and *HERC2* (**Supplementary Figure 4**).

### UM risk loci and pigmentation

To evaluate the impact of risk SNPs on gene regulation, eQTL analyses were performed for the statistically significant loci using expression data from tumors of an in-house series of 73 UMs (14). We previously identified an association between *CLPTM1L* expression and rs421284 with higher expression of *CLPTM1L* in individuals carrying the risk allele (C) (12). Interestingly, the other two major risk loci identified in this association study, *IRF4* and *HERC2*, are known to be strongly implicated in the regulation of the pigmentation



pathways determining eye and skin colors (15-17), prompting us to further investigate the expression of pigmentation genes in UM. *IRF4* expression was found to be strongly associated with rs12203592 alleles, with a decreased expression in tumors carrying the risk TT genotype (linear regression  $P = 2.00 \times 10^{-6}$ , **Supplementary Figure 5A**). Looking at eQTLs in the Genotype-Tissue Expression (GTEx) database, rs12203592 is linked to *IRF4* expression in most tissues, but the directionality of the association varies. As in UM, sun-exposed skin had a lower *IRF4* expression linked to the T allele, whereas a lower expression of *IRF4* is associated with the C allele in all other tissues, suggesting a tissue-specific regulation for this gene (**Supplementary Figure 5B**). At the *HERC2* locus, no correlation was found between rs12913832 alleles and expression of this gene in UM (**Supplementary Figure 6A**), in contrast to whole blood, where there is a statistically significant decrease in *HERC2* expression associated with the G allele (**Supplementary Figure 6B**). However, expression of *OCA2*, a nearby gene known to be regulated by *HERC2* in melanocytes (17), was found with a highly statistically significant association with rs12913832 genotypes ( $P = 9.08 \times 10^{-4}$ ) in UM, with decreased expression for tumors carrying the risk G allele (**Supplementary Figure 6C**).

Our finding of two major pigmentation loci is in accordance with the high prevalence of light eye color in UM patients of European ancestry (11). We investigated whether the risk of developing UM conferred by the risk alleles of *HERC2* and *IRF4* was fully linked to their determining role in eye pigmentation. We thus predicted the eye color of all UM and control individuals included in this study, using the algorithm developed in the IrisPlex System, based on the genotype combination of 6 SNPs (*HERC2* rs12913832, *OCA2* rs1800407, *SLC45A2* rs16891982, *TYR* rs1393350, *IRF4* rs12203592 and *LOC105370627*: intron variant) (18). We predicted the eye color of UM patients and controls to be either brown (41.6% of cases vs 60.1% of controls, respectively), green (1.7% vs 1.1%) or blue (56.7% vs 38.9%), allowing us to confirm the statistically significant association of blue eye color (versus other eye colors) with UM risk (OR=2.07, 95% CI = 1.72-2.49, 2-sided Fisher test

$P=1.21\times 10^{-15}$ ) (**Figures 3, A and B**), confirming the recent study by Jager and colleagues (19). Strikingly, when we added eye color (determined by the IrisPlex System) as a covariate in the association analysis, the resulting OR remained unchanged for *IRF4* (OR=1.76, 95% CI = 1.44-2.16, Firth logistic regression  $P=3.55\times 10^{-8}$  without eye color covariate; vs. OR=1.76, 95% CI = 1.43-2.17,  $P=9.25\times 10^{-8}$  with eye color covariate; **Figure 3C** and **Supplementary Table 4**). Conversely, the OR of *HERC2* risk SNP rs12913832 lost statistical significance with eye color covariate (OR=0.57, 95% CI = 0.48-0.67,  $P=1.88\times 10^{-11}$  without eye color covariate; vs. OR=0.76, 95% CI = 0.57-1.02,  $P=0.06$  with eye color covariate), in accordance with the major role of rs12913832 in the determination of eye pigmentation (17,18). As expected, the OR of *CLPTM1L*, a gene with no known role in pigmentation, remained unchanged (rs421284: OR=1.58, 95% CI = 1.35-1.86,  $P=1.98\times 10^{-8}$  without eye color covariate; vs. OR=1.58, 95% CI = 1.34-1.86,  $P=4.01\times 10^{-8}$  with eye color covariate; **Figure 3C, Supplementary Table 4**). This indicates that the implication of the *IRF4* locus in UM risk is not only explained by the prevalence of UM among individuals with light eye color, but also points towards another role for this risk locus beyond pigmentation.

### Pigmentation risk loci and UM epidemiology

The higher prevalence of UM among individuals of European ancestry strongly supports the existence of inherited risk alleles for the disease. The *TERT/CLPTM1L* risk locus does not account for this population bias, as the risk haplotype is more frequent in African American populations than those of European ancestry (rs421284, VAF=0.597 vs 0.429, respectively) (**Supplementary Table 5**, Genome Aggregation Database, GnomAD v2.1). However, the risk haplotypes of both *IRF4* and *HERC2* are found at statistically significantly higher frequencies in populations of Non-Finish European ancestry (NFE) than in those of African/ African-American (AFR) and East-Asian (EAS) origins (populations defined by gnomAD) (*IRF4* rs12203592, VAF=0.144, 0.034 and 0.000, respectively; *HERC2* rs12913832, VAF=0.803, 0.125 and 0.001, respectively (two-sided Fisher test  $P<1.00\times 10^{-20}$

for all statistical comparisons of NFE vs. EAS and NFE vs. AFR). Therefore, the higher frequency of the risk alleles of these two pigmentation loci may at least partly explain the higher prevalence of UM in European populations.

### Association study for the two major UM subtypes

Loss of chromosome 3 is the strongest factor associated with poor metastatic outcome in UM and correlates with increased mortality (2,3). The genomic status was available for 384 UM cases, allowing us to test for differential association of UM risk loci according to chromosome 3 status. Association studies were performed independently on UMs with D3 or M3 (246 M3 and 138 D3) vs. controls (CTL), for the most statistically significant SNP of each risk locus identified by GWAS (**Table 1**). Interestingly, rs12203592 (*IRF4* locus) showed a strong association with D3-UM, using a logistic regression model ( $OR_{D3vsCTL}=2.73$ , 95% CI = 1.87-3.97,  $P=1.78\times 10^{-7}$ ) whereas the association vanished completely in M3-UM ( $OR_{M3vsCTL}=1.01$ , 95% CI = 0.7-1.47,  $P=0.95$ ). On the contrary, rs12913832 (*HERC2* locus) showed a statistically significant high association with M3-UM, but not with D3-UM ( $OR_{M3vsCTL}=2.43$ , 95% CI = 1.79-3.29,  $P=1.13\times 10^{-8}$ ;  $OR_{D3vsCTL}=1.10$ , 95% CI = 0.80-1.52,  $P=0.56$ ). As for rs421284 (*CLPTM1L* locus), no preferential association was found in either UM subgroup ( $OR_{D3vsCTL}=2.26$ , 95% CI = 1.61-3.17,  $P=2.64\times 10^{-6}$ ;  $OR_{M3vsCTL}=1.55$ , 95% CI = 1.18-2.03,  $P=0.001$ ) (**Table 1**). To further assess the statistical significance of the observed differential association of rs12203592 in M3 and D3, we compared both subgroups ( $OR_{M3vsD3}$ ) for their association with UM risk SNPs (**Supplementary Table 6**). As expected, the OR of *CLPTM1L* rs421284 with M3- or D3-UMs collapsed towards the value 1, indicating that this SNP was similarly associated with both subgroups ( $OR_{M3vsD3}=0.86$ , 95% CI = 0.67-1.11,  $P=0.33$ ). Conversely, the low  $OR_{M3vsD3}$  and statistically significant  $P$  value obtained for *IRF4* rs12203592 ( $OR_{M3vsD3}=0.38$ , 95% CI = 0.27-0.52,  $P=8.46\times 10^{-7}$ ) and the high  $OR_{M3vsD3}$  for *HERC2* rs12913832 ( $OR_{M3vsD3}=1.81$ , 95%

CI = 1.38-2.38,  $P = 3.87 \times 10^{-4}$ ) recapitulated the specific association of these risk regions for D3- and M3-UM, respectively.

These data strongly suggest that UM tumor biology is influenced by the genetic background predisposing to UM, with *CLPTM1L* SNPs predisposing to all UM types, *IRF4* SNP predisposing specifically to risk in D3-UM and *HERC2* locus to risk in M3-UM.

## Discussion

We extended our initial UM GWAS by including a total of 1,142 UM cases and by performing genome-wide genotype imputation. This allowed us to recapitulate the previously described *CLPTM1L* risk locus, and to further identify *IRF4* and *HERC2*, two pigmentation loci, as UM genetic risk factors. Furthermore, we demonstrated that while *CLPTM1L* is a risk locus in all UM subgroups, *IRF4* is specifically associated with D3-UM and *HERC2* specifically with M3-UM.

The *TERT/CLPTM1L* region has frequently been associated in GWAS studies, with higher and lower tumor risk depending on cancer types (20). The function of *CLPTM1L* is not yet fully understood but this protein is thought to contribute to RAS-dependent transformation and tumorigenesis, including in pancreatic tumorigenesis (21-23). On the other hand, *TERT* (on the same locus) plays a major role in telomere maintenance (24). In a previous study, we revealed a correlation between rs421284 genotype and *CLPTM1L* expression but not *TERT*, the latter being poorly expressed in UMs (12). Whether *CLPTM1L* or *TERT* is the target of this risk haplotype in UM tumorigenesis is still unclear.

We confirmed the association of the *OCA2/HERC2* locus with UM risk, initially identified as candidate SNPs by Ferguson *et al.* (25). We confirmed the correlation between *HERC2* rs12913832 and *OCA2* expression in UM, with a decreased expression in individuals carrying the G allele (**Supplementary Figure 6C**). *HERC2* is known to regulate the expression of *OCA2*, which codes for a protein involved in determining the melanin type

and amount (26). These two genes are the main genetic determinants of iris color (18). In melanocytic cell lines, the transcription factor HLTF binds to the A but not the G allele of rs12913832, creating an activating loop for *OCA2* transcription by the recruitment of MITF and LEF1 (17,27). The rs12913832 A allele is consequently associated with high expression of *OCA2*, production of melanin, brown eye color and low UM risk, and conversely for the rs12913832 G allele.

The third UM risk locus identified in the present study is characterized by a single risk SNP on *IRF4*, rs12203592 (25). *IRF4* regulates the expression of key pigmentation genes in association with MITF, including *TYR* involved in the production of melanin. The *IRF4* locus is also associated with melanocytic naevus count, freckling and tanning ability (28-30). TFAP2 $\alpha$  recognizes rs12203592 C allele in melanocytes, allowing the recruitment of MITF, YY1 and potentially LEF1, and increasing *IRF4* expression (15,16). Conversely, rs12203592 T allele prevents TFAP2 $\alpha$  binding resulting in lower *IRF4* expression. We showed that the rs12203592 UM risk allele T is associated with a dramatic decreased expression of *IRF4* (**Supplementary Figure 5A**). Of note, only a minority of individuals (three in our in-house series) carry the TT genotype. A similar eQTL pattern was reported in sun-exposed skin from GTEX, whereas an opposite direction was found in other tissues (**Supplementary Figure 5B**), strongly suggesting that *IRF4* is regulated in a tissue-specific manner.

The present GWAS demonstrates the role of two pigmentation genes in the genetic risk of UM, in addition to the *CLPTM1L/TERT* risk locus. This is consistent with light iris color being a risk factor for UM (OR=1.75) (11,19,31) similar to our finding (OR=2.07). Iris pigmentation depends on the production and maturation of melanin as well as on the ratio of the two types of melanin, eumelanin (black-brown, densely packed) and pheomelanin (yellow-to-red, loosely packed). Melanin plays a major role protecting against ultra-violet radiation (UVR) by absorbing free radicals and inhibiting UV-mediated damage (32). Pheomelanin, however, can also induce more oxidative damage upon UVR than eumelanin (33), which was proposed to explain the contribution of light iris color in UM (34). However,

the steady UM incidence despite increased UVR exposure, the low tumor mutation burden and absence of UVR mutational signature in UM tumors ruled out this hypothesis (5,35). Interestingly, iris melanoma, a rare form of UM, is associated with high tumor mutation burden and a UVR signature (36); consistent with iris color being a risk factor for iris melanoma (37). However, our GWAS is restricted to choroid melanoma, a tissue that, unlike the iris, is not directly exposed to sunlight. In this respect, iris color could also be a surrogate marker for other phenomena, and *IRF4*, and also potentially *HERC2/OCA2*, SNPs may also play a role outside from pigmentation to explain UM risk. However, a limitation of our study is that eye pigmentation is deduced from genotypes, which are also risk SNPs for UM, making it challenging to derive causal statements.

Status of chromosome 3 and *BAP1* delineates two UM subtypes, M3/*BAP1* inactivated ‘high-risk’ tumors and D3/wild-type *BAP1* ‘low-risk’ tumors (2-4,8). Strikingly, while *CLPTM1L* region confers similar susceptibility for M3- and D3-UM, we show that the risk for M3-UM is associated with the *OCA2/HERC2* region, and D3-UM with the *IRF4* locus. How these processes influence the malignant transformation is unknown, but most probably independent of the protective role of melanin against UVR. Furthermore, our data reinforces the idea that UM encompasses at least two diseases, with distinct clinico-biological characteristics (8,38-40), and distinct susceptibility loci.

Further studies should investigate the molecular mechanisms behind these UM genetic susceptibility loci to understand the role of pigmentation genes in UM risk. This study provides important insights in the genetics of UM and may lead to improvements in risk prediction and to a better understanding of the biological basis of UM.

## Funding

A.-.C. D. was supported by the Horizon 2020 program and innovation program under the Marie Skłodowska-Curie grant agreement No 666003 and the Ligue Nationale Contre le

Cancer. L.M. was supported by the Horizon 2020 program UM Cure (No 667787). This study was funded by the INCa *Programme de recherche sur le cancer en Sciences Humaines et Sociales, Epidémiologie et Santé Publique* (2017-1-PL SHS-02), the Horizon 2020 program UM Cure (No 667787), the Institut National de la Santé et de la Recherche Médicale (INSERM), the Institut Curie, the Ligue Nationale Contre le Cancer (Labellisation) and the *Site de Recherche Intégrée sur le Cancer* (SiRIC2) de l'Institut Curie. Genome-wide genotyping of the French controls including in the KIDRISK study was founded by the US National Institutes of Health (NIH), National Cancer Institute (U01CA155309) through the IARC-2 scan.

## Notes

**Role of the funder:** The funders had no role in the design of the study; the collection, analysis, and interpretation of the data; the writing of the manuscript; and the decision to submit the manuscript for publication.

**Disclosures:** The authors have no conflict of interest to declare.

**Author contributions:** L.M, A-C.D. and A.H contributed equally to this study. L.M, A-C.D, A.H and M-H.S. conceptualized the study and developed its methodology. G. C-T, O.C. and G.S. provided resources (GWAS control samples). A-C.D., L.M., A.B.,J.-F.D. conducted research investigation (experiments). L.M, A.H, T.V. and J.N. performed data curation and formal analysis. G.P., N.C. and M.M. provided resources. A-C.D, A.H. and L.M conducted experiments, performed visualization/data presentation, and wrote and edited the manuscript. G.C., M.R., J.N. and M.R. reviewed the manuscript. M-H.S. supervised the study. All authors reviewed and approved the final manuscript.

**Acknowledgements:** Authors are grateful to the patients for accepting to participate in this study. The authors would like to thank Antoine Chouteau, Manon Reverdy, Marion Gautier and Khadija Ait Rais for their help in managing samples and are grateful for the Biological Resource Center of the Institut Curie and its members for preparing patients' DNAs.

## Data Availability

Dataset2 and 3 genotyping data used in the analysis are have been deposited and are available on the European Genome-Phenome Archive (EGA) (<https://ega-archive.org/>) under accession number EGAS00001005200. Previously published genotyping of dataset1 cases and controls are found on EGA under Accession number EGAS00001002334 and on the database for Genotypes and Phenotypes (dbGaP) under accession number phs001271.v1.p1., respectively. Previously published expression data (RNA-seq data) of 73 UM tumors are available at EGA under accession no. EGAS00001002932). PCAs were performed using HapMap3 ([ftp://ftp.ncbi.nlm.nih.gov/hapmap/genotypes/hapmap3\\_r3](ftp://ftp.ncbi.nlm.nih.gov/hapmap/genotypes/hapmap3_r3)). For expression quantitative trait loci (eQTL) analyses, data was obtained from the Genotype-Tissue Expression (GTEx) public database (<https://www.gtexportal.org/home/>). Allele frequency of SNPs of interest in different populations was obtained from the Genome Aggregation Database (GnomAD v2.1.1, <https://gnomad.broadinstitute.org>).

Code availability: The following web-based resources were used in the GWAS analysis: PLINK 1.9 and 2.0 (<https://www.cog-genomics.org/plink/1.9/> , <https://www.cog-genomics.org/plink/2.0/>), Michigan Imputation Server (<https://imputationserver.sph.umich.edu/index.html>), GitHub (<https://github.com/DReichLab/EIG>), and HIRISplex (<https://hirisplex.erasmusmc.nl/>). The code generated during this study is available at [https://gitlab.curie.fr/ahouy/gwas/-/blob/master/GWAS\\_analysis.html](https://gitlab.curie.fr/ahouy/gwas/-/blob/master/GWAS_analysis.html).

## References



1. Jager MJ, Shields CL, Cebulla CM, *et al.* Uveal melanoma. *Nat Rev Dis Primers* 2020;6(1):24.
2. Singh AD, Aronow ME, Sun Y, *et al.* Chromosome 3 status in uveal melanoma: a comparison of fluorescence in situ hybridization and single-nucleotide polymorphism array. *Invest Ophthalmol Vis Sci* 2012;53(7):3331-9.
3. Cassoux N, Rodrigues MJ, Plancher C, *et al.* Genome-wide profiling is a clinically relevant and affordable prognostic test in posterior uveal melanoma. *Br J Ophthalmol* 2014;98(6):769-74.
4. Harbour JW, Onken MD, Roberson ED, *et al.* Frequent mutation of BAP1 in metastasizing uveal melanomas. *Science* 2010;330(6009):1410-3.
5. Furney SJ, Pedersen M, Gentien D, *et al.* SF3B1 mutations are associated with alternative splicing in uveal melanoma. *Cancer Discov* 2013;3(10):1122-1129.
6. Harbour JW, Roberson ED, Anbunathan H, *et al.* Recurrent mutations at codon 625 of the splicing factor SF3B1 in uveal melanoma. *Nat Genet* 2013;45(2):133-5.
7. Martin M, Masshofer L, Temming P, *et al.* Exome sequencing identifies recurrent somatic mutations in EIF1AX and SF3B1 in uveal melanoma with disomy 3. *Nat Genet* 2013;45(8):933-6.
8. Robertson AG, Shih J, Yau C, *et al.* Integrative Analysis Identifies Four Molecular and Clinical Subsets in Uveal Melanoma. *Cancer Cell* 2017;32(2):204-220 e15.
9. Aronow ME, Topham AK, Singh AD. Uveal Melanoma: 5-Year Update on Incidence, Treatment, and Survival (SEER 1973-2013). *Ocul Oncol Pathol* 2018;4(3):145-151.
10. Bishop KD, Olszewski AJ. Epidemiology and survival outcomes of ocular and mucosal melanomas: a population-based analysis. *Int J Cancer* 2014;134(12):2961-71.
11. Weis E, Shah CP, Lajous M, *et al.* The association between host susceptibility factors and uveal melanoma: a meta-analysis. *Arch Ophthalmol* 2006;124(1):54-60.
12. Mobuchon L, Battistella A, Bardel C, *et al.* A GWAS in uveal melanoma identifies risk polymorphisms in the CLPTM1L locus. *NPJ Genom Med* 2017;2(1):5.

13. Thomsen H, Chattopadhyay S, Hoffmann P, *et al.* Genome-wide study on uveal melanoma patients finds association to DNA repair gene TDP1. *Melanoma Res* 2019; 10.1097/CMR.0000000000000641.
14. Alsafadi S, Houy A, Battistella A, *et al.* Cancer-associated SF3B1 mutations affect alternative splicing by promoting alternative branchpoint usage. *Nat Commun* 2016;7:10615.
15. Visser M, Palstra RJ, Kayser M. Allele-specific transcriptional regulation of IRF4 in melanocytes is mediated by chromatin looping of the intronic rs12203592 enhancer to the IRF4 promoter. *Hum Mol Genet* 2015;24(9):2649-61.
16. Praetorius C, Grill C, Stacey SN, *et al.* A polymorphism in IRF4 affects human pigmentation through a tyrosinase-dependent MITF/TFAP2A pathway. *Cell* 2013;155(5):1022-33.
17. Visser M, Kayser M, Palstra RJ. HERC2 rs12913832 modulates human pigmentation by attenuating chromatin-loop formation between a long-range enhancer and the OCA2 promoter. *Genome Res* 2012;22(3):446-55.
18. Walsh S, Liu F, Ballantyne KN, *et al.* IrisPlex: a sensitive DNA tool for accurate prediction of blue and brown eye colour in the absence of ancestry information. *Forensic Sci Int Genet* 2011;5(3):170-80.
19. Houtzagars LE, Wierenga APA, Ruys AAM, *et al.* Iris Colour and the Risk of Developing Uveal Melanoma. *Int J Mol Sci* 2020;21(19).
20. Wang Z, Zhu B, Zhang M, *et al.* Imputation and subset-based association analysis across different cancer types identifies multiple independent risk loci in the TERT-CLPTM1L region on chromosome 5p15.33. *Hum Mol Genet* 2014;23(24):6616-33.
21. James MA, Vikis HG, Tate E, *et al.* CRR9/CLPTM1L regulates cell survival signaling and is required for Ras transformation and lung tumorigenesis. *Cancer Res* 2014;74(4):1116-27.
22. Jia J, Bosley AD, Thompson A, *et al.* CLPTM1L promotes growth and enhances aneuploidy in pancreatic cancer cells. *Cancer Res* 2014;74(10):2785-95.

23. Clarke WR, Amundadottir L, James MA. CLPTM1L/CRR9 ectodomain interaction with GRP78 at the cell surface signals for survival and chemoresistance upon ER stress in pancreatic adenocarcinoma cells. *Int J Cancer* 2019;144(6):1367-1378.
24. Shay JW, Wright WE. Telomeres and telomerase: three decades of progress. *Nat Rev Genet* 2019;20(5):299-309.
25. Ferguson R, Vogelsang M, Ucisik-Akkaya E, *et al.* Genetic markers of pigmentation are novel risk loci for uveal melanoma. *Sci Rep* 2016;6:31191.
26. Frudakis T, Terravainen T, Thomas M. Multilocus OCA2 genotypes specify human iris colors. *Hum Genet* 2007;122(3-4):311-26.
27. Sturm RA, Larsson M. Genetics of human iris colour and patterns. *Pigment Cell Melanoma Res* 2009;22(5):544-62.
28. Ainger SA, Jagirdar K, Lee KJ, *et al.* Skin Pigmentation Genetics for the Clinic. *Dermatology* 2017;233(1):1-15.
29. Duffy DL, Iles MM, Glass D, *et al.* IRF4 variants have age-specific effects on nevus count and predispose to melanoma. *Am J Hum Genet* 2010;87(1):6-16.
30. Han J, Qureshi AA, Nan H, *et al.* A germline variant in the interferon regulatory factor 4 gene as a novel skin cancer risk locus. *Cancer Res* 2011;71(5):1533-9.
31. Schmidt-Pokrzywniak A, Jockel KH, Bornfeld N, *et al.* Positive interaction between light iris color and ultraviolet radiation in relation to the risk of uveal melanoma: a case-control study. *Ophthalmology* 2009;116(2):340-8.
32. Krol ES, Liebler DC. Photoprotective actions of natural and synthetic melanins. *Chem Res Toxicol* 1998;11(12):1434-40.
33. Ye T, Hong L, Garguilo J, *et al.* Photoionization thresholds of melanins obtained from free electron laser-photoelectron emission microscopy, femtosecond transient absorption spectroscopy and electron paramagnetic resonance measurements of oxygen photoconsumption. *Photochem Photobiol* 2006;82(3):733-7.

34. d'Ischia M, Wakamatsu K, Cicoira F, *et al.* Melanins and melanogenesis: from pigment cells to human health and technological applications. *Pigment Cell Melanoma Res* 2015;28(5):520-44.
35. Royer-Bertrand B, Torsello M, Rimoldi D, *et al.* Comprehensive Genetic Landscape of Uveal Melanoma by Whole-Genome Sequencing. *Am J Hum Genet* 2016;99(5):1190-1198.
36. Johansson PA, Brooks K, Newell F, *et al.* Whole genome landscapes of uveal melanoma show an ultraviolet radiation signature in iris tumours. *Nat Commun* 2020;11(1):2408.
37. Rootman J, Gallagher RP. Color as a risk factor in iris melanoma. *Am J Ophthalmol* 1984;98(5):558-61.
38. Durante MA, Rodriguez DA, Kurtenbach S, *et al.* Single-cell analysis reveals new evolutionary complexity in uveal melanoma. *Nat Commun* 2020;11(1):496.
39. Field MG, Kuznetsov JN, Bussies PL, *et al.* BAP1 Loss Is Associated with DNA Methylomic Repatterning in Highly Aggressive Class 2 Uveal Melanomas. *Clin Cancer Res* 2019;25(18):5663-5673.
40. Onken MD, Worley LA, Ehlers JP, *et al.* Gene expression profiling in uveal melanoma reveals two molecular classes and predicts metastatic death. *Cancer Res* 2004;64(20):7205-9.

## Table

**Table 1. Main risk loci in uveal melanoma according to their chromosome 3 status.**

ID <sup>a</sup>	SNP <sup>b</sup>	Symbol	Alternative allele	Monosomy 3			Disomy 3		
				Total No. (cases/controls)	OR (95% CI)	<i>P</i> <sup>c</sup>	Total No. (cases/controls)	OR (95% CI)	<i>P</i> <sup>c</sup>
5:1325590:T>C	rs421284	<i>CLPTM1L</i>	C	1126 (244/882)	1.55 (1.18-2.03)	0.001	1018 (137/881)	2.26 (1.61-3.17)	2.64x10 <sup>-6</sup>
6:396321:C>T	rs12203592	<i>IRF4</i>	T	1126 (244/882)	1.01 (0.70-1.47)	0.95	1018 (137/881)	2.73 (1.87-3.97)	1.78x10 <sup>-7</sup>
15:28365618:A>G	rs12913832	<i>HERC2</i>	G	1126 (244/882)	2.43 (1.79-3.29)	1.13x10 <sup>-8</sup>	1018 (137/881)	1.10 (0.80-1.52)	0.56

<sup>a</sup>ID refers to chromosome number : chromosomal genomic position : reference allele > alternative allele, based on genome build GRCh37 (hg19). CI = confidence interval; OR = odds ratio.

<sup>b</sup>SNP = single nucleotide polymorphism, according to The Single Nucleotide Polymorphism Database (dbSNP).

<sup>c</sup>Two-sided *P* values were calculated by general linear model (GLM).

## Figure titles and legends

**Figure 1: Files and pipeline used for the filtering and imputation of the Genome-Wide Association Study in uveal melanoma.** SNP = single nucleotide polymorphism.

**Figure 2: Manhattan plot and regional linkage disequilibrium plot for statistically significant loci.** For the Manhattan plot, the association test  $P$  value (y-axis) is plotted against its physical chromosomal position (x-axis). Chromosomes are shown in alternating black and grey. SNPs above the top horizontal line represent those with a  $P$  value  $<5.00 \times 10^{-8}$  and were considered to be statistically significantly associated with uveal melanoma. The bottom horizontal line represents the tendency line ( $P$  value  $<1.00 \times 10^{-5}$ ). Statistical significance was measured using unconditional logistic regressions. For regional locus plots, genes are depicted with rectangles and SNPs are represented by dots. Shading of dots reflects the level of linkage disequilibrium ( $r^2$ ) with the highlighted SNP of interest (black circle with rs number indicated). Vertical bars indicate recombination rates in human population. SLC12A7: solute carrier family 12 member 7; SLC6A19: solute carrier family 6 member 19; SLC6A18: solute carrier family 6 member 18; TERT: telomerase reverse transcriptase; CLPTM1L: cleft lip and palate transmembrane protein 1-like; SLC6A3: solute carrier family 6 member 3; LPCAT1: lysophosphatidylcholine acyltransferase 1; DUSP22: dual specificity phosphatase 22; IRF4: interferon regulatory factor 4; EXOC2: exocyst complex component 2; OCA2: oculocutaneous albinism II; HERC2: HECT and RLD domain containing E3 ubiquitin protein ligase 2.

**Figure 3: Eye pigmentation and uveal melanoma risk. (A)** Proportion of blue, green and brown eye colors among uveal melanoma (UM) cases (dark shade) and controls (light shade), as predicted by the IrisPlex System (18). **(B)** Proportion of blue eyes versus other eye colors

in UM cases and controls. The number of individuals is indicated. The association of blue eye color with UM risk is indicated by the Fisher test p-value and odds ratio (OR). The 95% confidence interval for the odds ratio is indicated within brackets. **(C)** Effect of eye color as a GWAS covariate on the odds ratio (OR) for the 3 main SNPs of statistically significant UM risk loci (*CLPTM1L*, *IRF4* and *HERC2*). The error bars indicate the 95% confidence intervals for the odds ratio. Statistical significance was assessed using a two-sided Fisher test. The + and - indicate the inclusion or exclusion of eye color as a GWAS covariate, respectively. For each SNP and in both covariate conditions, association with UM risk is represented by the OR (x-axis) and associated *P* value. The vertical dotted line is set at OR = 1.00, indicating an absence of association with UM. All statistical tests were 2-sided. OR: odds ratio; *CLPTM1L*: cleft lip and palate transmembrane protein 1-like; *IRF4*: interferon regulatory factor 4; *HERC2*: HECT and RLD domain containing E3 ubiquitin protein ligase 2.

**Figure 1**

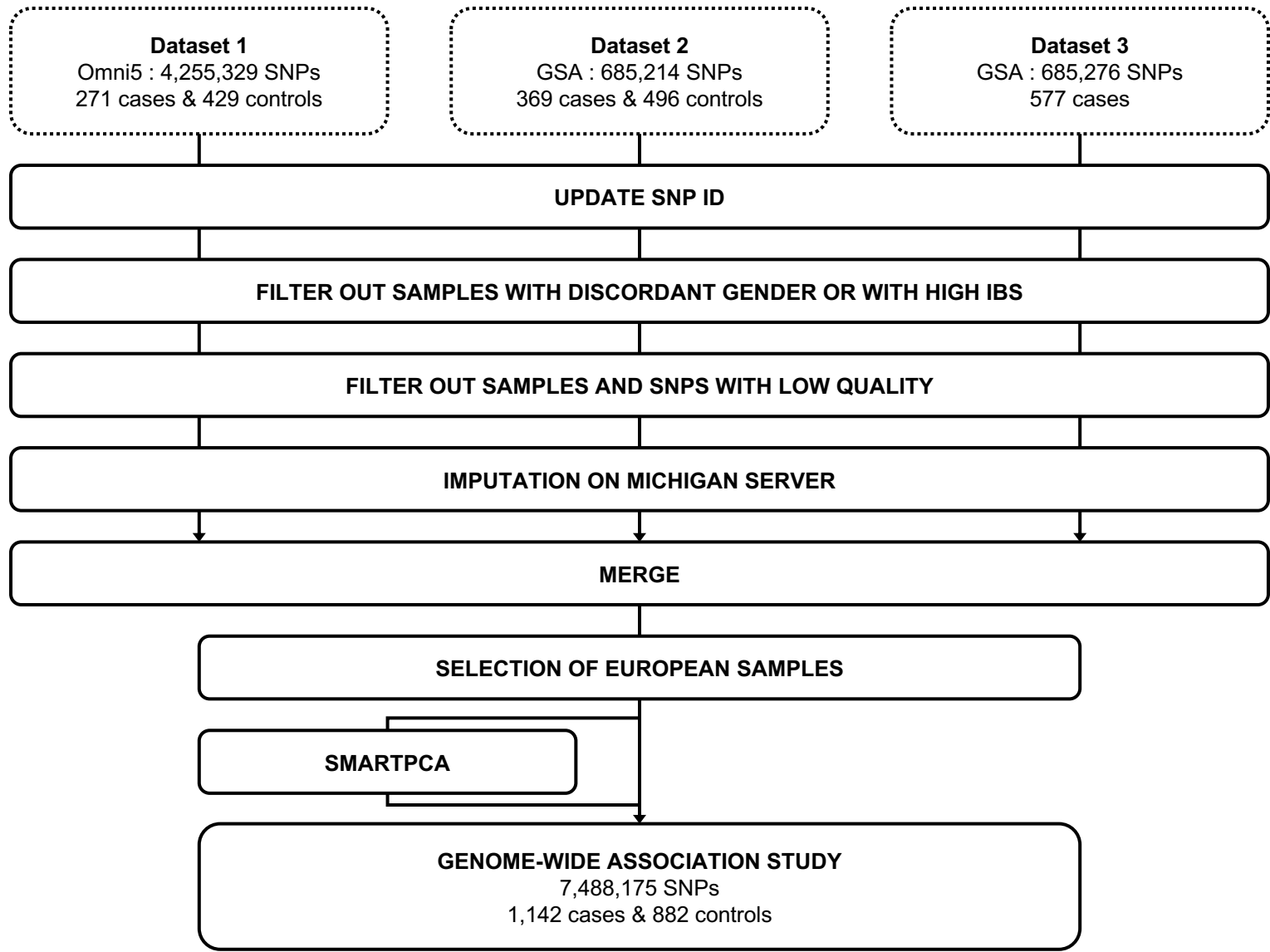
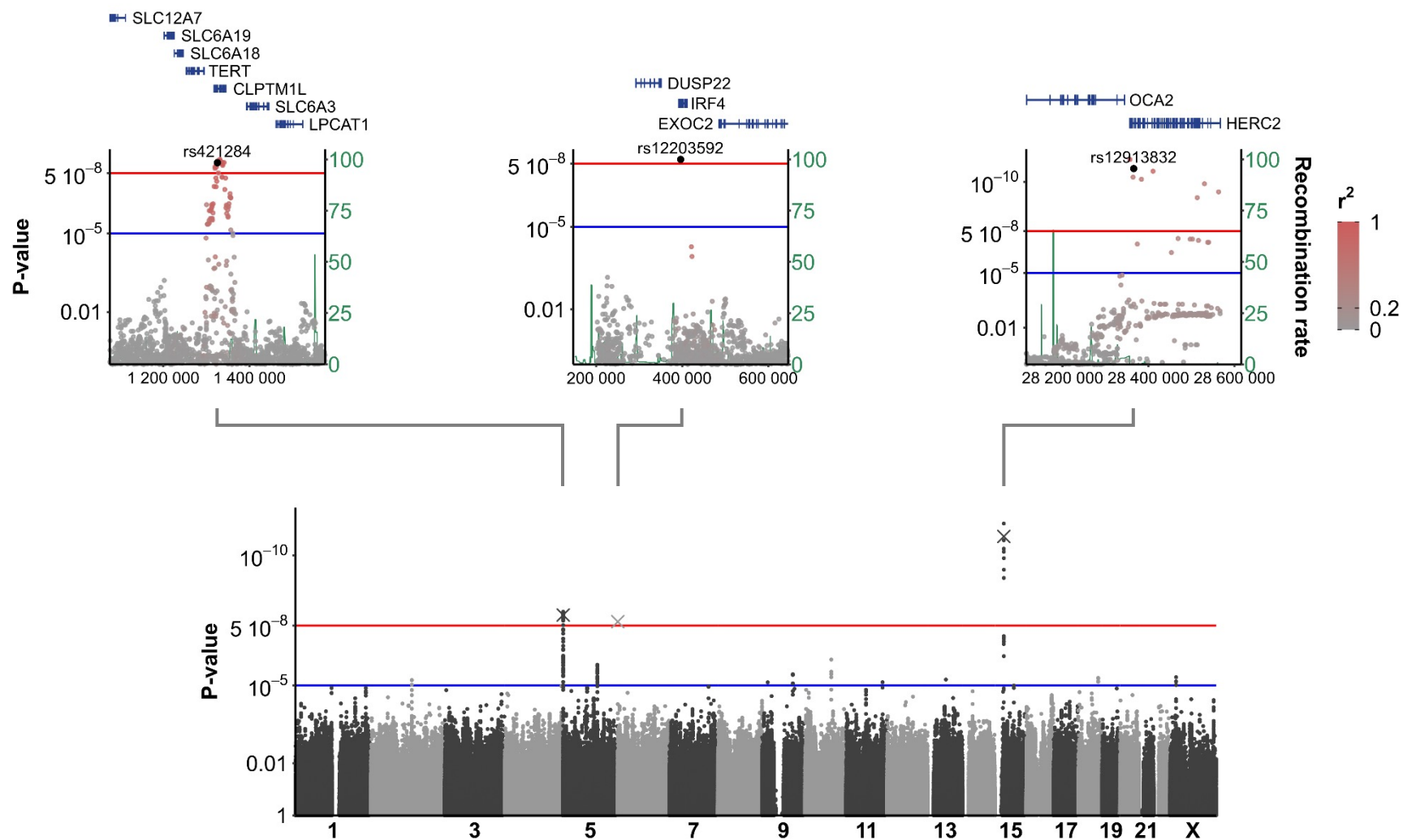




Figure 2



**Figure 2**

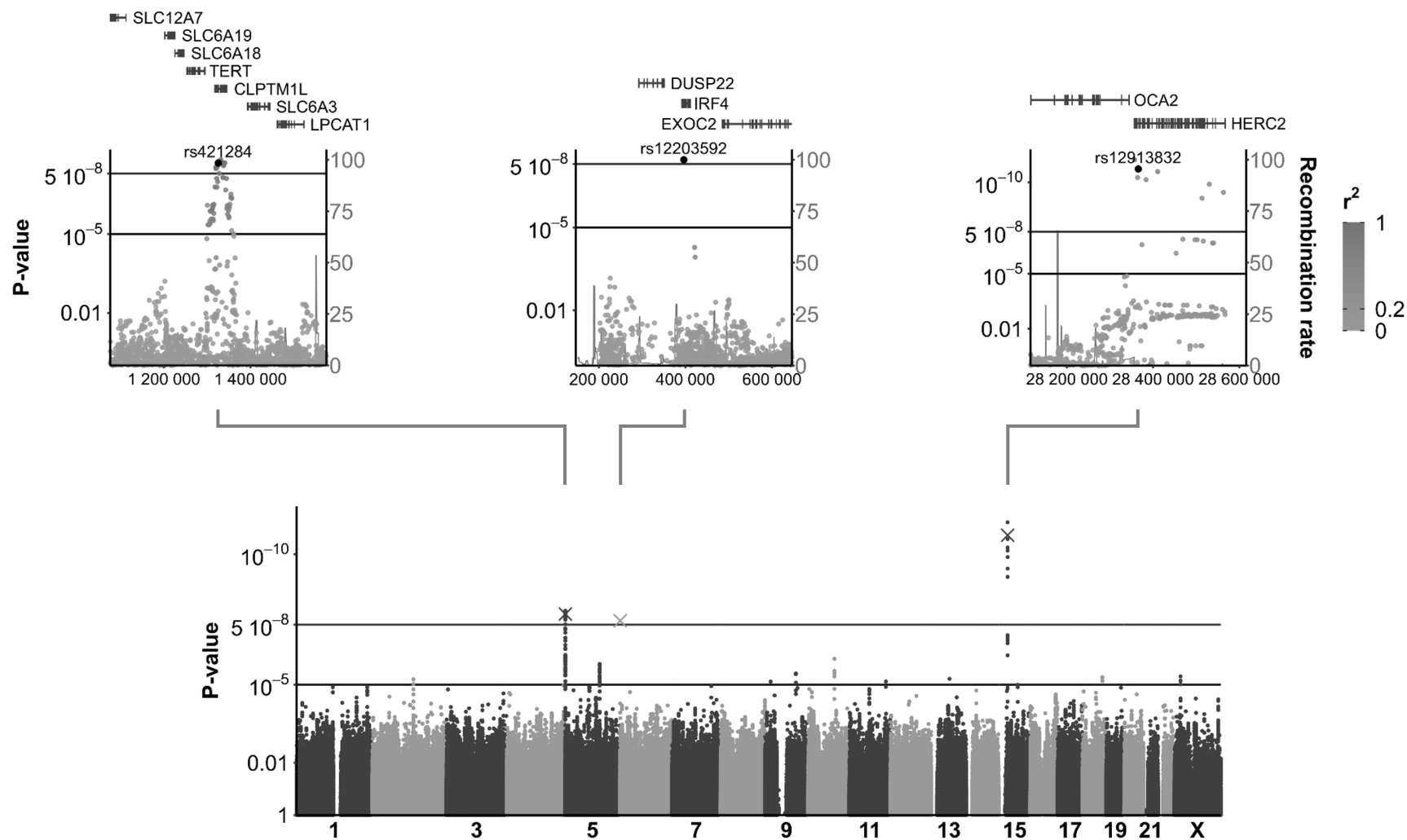


Figure 3

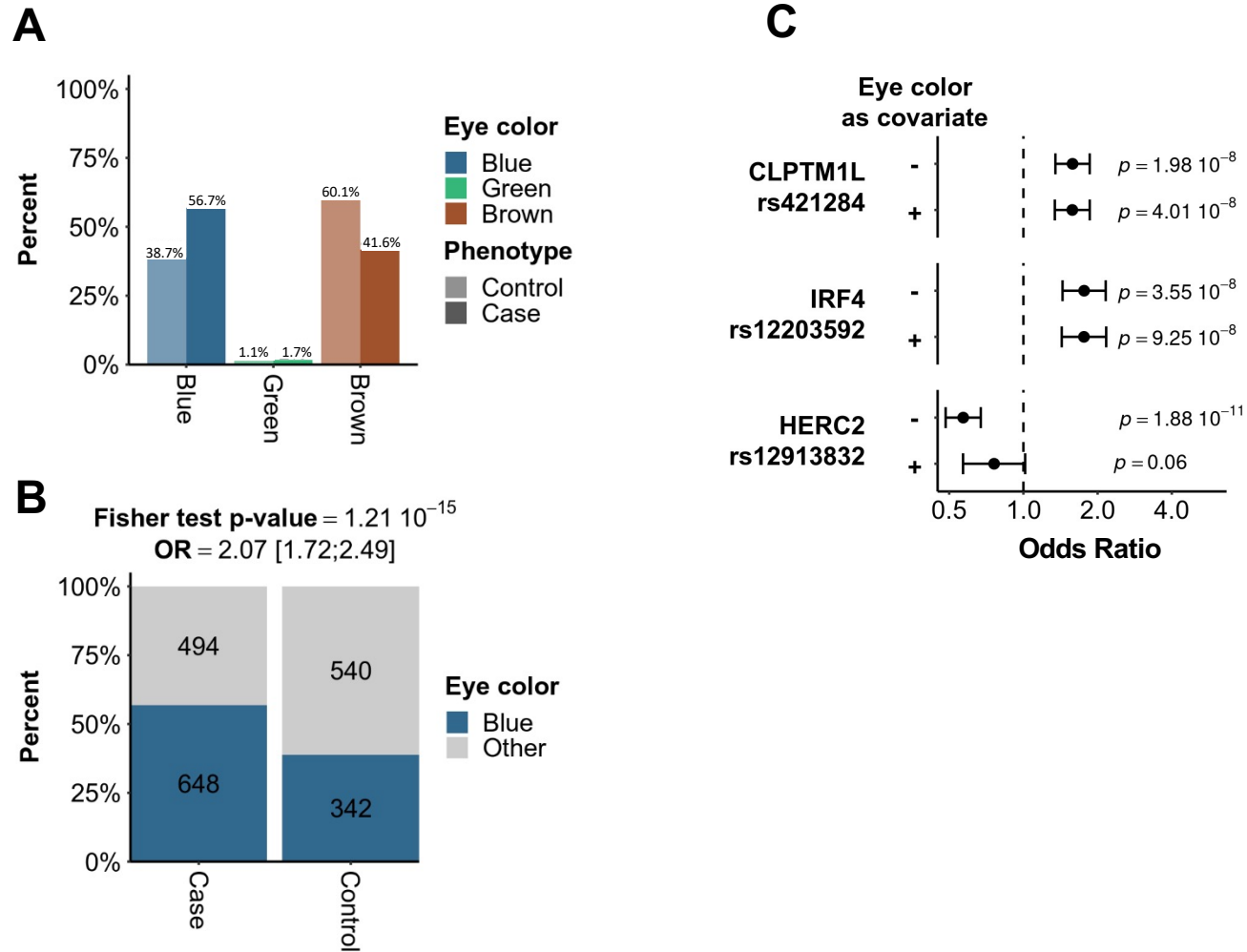


Figure 3

